Hypoxia induces chemoresistance to proteasome inhibitors through orchestrating deSUMOylation and ubiquitination of SRC-3 in multiple myeloma

zhiqiang Liu (zhiqiangliu@tmu.edu.cn)
Tianjin Medical University https://orcid.org/0000-0002-0677-8097
Jing Guo
Tianjin Medical University
Yangyang Lv
Sheng Wang
Ziyi Peng
Tianjin Medical University
Ying Xie
Tianjin Medical University
Yixuan Wang
Tianjin Medical University
Hongmei Jiang
Tianjin Medical University
Xin Li
Tianjin Medical University
Qimeng Wang
Tianjin Medical University
Meilin Hu
Jiangpeng Mu
Jingya Wang
Tianjin Medical University
Yangyang Xie
Xiankui Cheng
Zhigang Zhao

Article

Keywords: Multiple myeloma, Chemoresistance, Hypoxia, SUMOylation, SRC-3, SENP1

Posted Date: May 31st, 2022

DOI: https://doi.org/10.21203/rs.3.rs-1658047/v1

Version of Record: A version of this preprint was published at Oncogene on October 8th, 2022. See the published version at https://doi.org/10.1038/s41388-022-02494-5.

Abstract

The bone marrow microenvironment where multiple myeloma (MM) originated is hypoxic and an important stimulus for initiation of drug resistance to chemotherapies, but the underlying mechanisms and key regulators are still indistinct. In the current study, we found that hypoxia stimulus easily induced chemoresistance to proteasome inhibitors (PIs) but not to other chemicals, and the steroid receptor coactivator 3 (SRC-3) expression was remarkably augmented at posttranslational level. Protein interactome analysis identified SENP1 as a key modifier of SRC-3 stability, as deSUMOylation by SENP1 attenuated the K11-linked polyubiquitination of SRC-3. Depletion of SENP1 in MM cells by CRISPR/cas9 sgRNA, or in $SENP1^{fl/fl}CD19^{Cre/+}$ B cells, accelerated the degradation of SRC-3, and overcame the resistance to PIs at vast scale, which phenotype was similar to administration of SENP1inhibitor Momordin Ic (Mc) in the Vk*Myc and 5TGM1 mouse models and patient derived xenograft (PDX) of myeloma. Importantly, SENP1 level was positively correlated with SRC-3 level in the tissues from refractory/relapsed MM, as well as in xenograft tissues from mice treated with bortezomib and Mc. Taken together, our findings suggest that hypoxia induced SENP1 is a crucial regulator of chemoresistance to PIs, and shed light on developing therapeutic strategies to overcome chemoresistance by using small molecules targeting SENP1 or SRC-3.

Introduction

Multiple myeloma (MM) is a hematologic malignancy of abnormal monoclonal plasma cells accumulating mainly in the bone marrow, and results in secretion of excessive parafunctional monoclonal immunoglobulin protein and end-organ damage.[1] The investigations in molecular mechanisms on bench and the successful application of proteasome inhibitors in the clinic have led to the significant overall survival of MM treatment.[2,3] However, MM remains incurable and fatal, which is mainly attributed to the occurrence of drug-resistant subclones during therapy.[4] A better understanding of the mechanisms by which drug resistance is caused is urgently required.

MM cells originate and reside in the bone marrow (BM) microenvironment, in which may contain a myeloma cell fraction that has acquired treatment resistance.[5] It has been reported that the BM niche confers survival and chemoresistance of MM cells to chemotherapies by a complex interplay of cytokines, chemokines, adhesion molecules, proteolytic enzymes and other components of the extracellular matrix.[6–8] Besides, BM has long been accepted to be a naturally hypoxic organ.[9,10] A study using the 5T33 MM murine model found that the myelomatous BM environment was more hypoxic than the normal BM microenvironment.[11] With progression of MM disease, BM niche undergoes fluctuating hypoxia and has strong selective pressure to tumor cell subsets that are able to adapt quickly to reduced oxygen availability.[12] Consequently, MM cells that adapt to hypoxia are highly aggressive, resistant to treatment and associated with a poor prognosis. For instance, our previous study revealed that hypoxia promotes disease progression and bone lesion through upregulates DKK1 expression.[13] Given that hypoxia promotes numerous aspects of tumor progression in solid malignancies, for example, live and

breast cancers,[14,15] it is likely that MM biology are strongly influenced by hypoxia. However, the mechanism of hypoxia induced MM drug resistance is still elusive, and it is pivotal in highlighting the importance of investigating the roles and mechanisms of hypoxia in the pathogenesis and chemoresistance of MM.

Highly dynamic post-translational modifications (PTMs) controlling accumulation and functions of proteins are pivotal for carcinogenesis and disease progression, including acetylation, phosphorylation, methylation, ubiquitination, SUMOylation, and NEDDylation.[16,17] Actually, post-translational modifications such as ubiquitination and SUMOylation play even critical roles in MM, since the most highly effective drugs for management of MM in clinic, such as proteasome inhibitors (PIs) and immunomodulatory drugs (iMiDs), disturb the ubiquitin-proteasome system, thus control NF-κB signaling, epigenetic regulations, DNA damage repair, and drug resistance.[18] For example, we have discovered that in the t(4;14) positive MM cells histone methyltransferase NSD2 stabilizes the steroid receptor coactivator-3 (SRC-3) to prevent degradation of SRC-3 and enhance chemoresistance.[19] In addition, ubiquitination and SUMOylation modification also regulates both the cellular concentrations and the co-activator activities of SRC-3. Wu *et al* reported that estrogen treatment led to decreased SUMOylation and increased phosphorylation in regulating the transcriptional activity of SRC-3[20]. However, key regulators of SRC-3 and the degradation machinery in the development of chemoresistance in MM cells, especially under the hypoxic conditions in the BM environment, are still not well elucidated. Thus, interpretation of these questions will facilitate the better understanding of molecular aspect of MM progression, and develop new strategies to overcome refractory or replace in the clinic.

In this study, we investigated the effect of hypoxia on chemosensitivity to proteasome inhibitors in MM cells through SENP1-mediated modification of SRC-3 protein, and evaluated the efficacy of newly developed SENP1 and SRC-3 inhibitors in overcoming chemoresistance on immortalized MM cell lines and on 5TGM1 and Vk*MYC mouse model of MM.

Materials And Methods

Ethics approval and consent to participate

This study was approved by the Ethics Committee of Tianjin Medical University, and all protocols conformed to the Ethical Guidelines of the World Medical Association Declaration of Helsinki. Signed informed consent was obtained from each participating individual prior to participation in the study. All Animal studies performed during this experiment were approved by the Committee on Animal Research and Ethics of Tianjin Medical University, and all protocols followed conformed with the Guidelines of Ethical Conduct in the Care and Use of Nonhuman Animals in Research.

Patient derived xenograft (PDX) mouse model for MM

To develop a PDX model, unsorted bone marrow mononuclear cells containing 0.5~1´10^6 $CD138^+$ from relapsed MM after bortezomib-based regimen treatment were implanted by intratibial drug administration (i.t.) into NSG mice (n = 6 mice/per patient). Recipient mice were bled weekly after inoculation in order to monitor engraftment. This was detected by the use of immunoglobulin ELISA Kits (ThermoFisher). Twice a week for three weeks from the 2^{nd} week after inoculation, solo bortezomib or in combination with Mc was administered, and the human $CD138^+$ cells from mice bone marrow were analyzed by flow cytometry after the treatments were completed.

Vk*Myc transgenic and transplant mouse models of MM

The Vk*Myc transgenic and transplant mouse model were established according to Dr. Bergsagel PL's report.[21] Briefly, 0.5´10^6 cells/mouse were injected via tail vein of 5- to 12-week-old C57BL/6 wild-type recipient mice. 1 Week after transplantation for SPEP analysis, recipient mice were bled weekly. Their time to engraftment (TTE), or time to first appearance of the M-protein spike, was calculated by the Kaplan-Meier survival curve and log-rank test.

Statistical analysis

Data were shown as mean ± SD for at least n=3 independent experiments except otherwise explanation. Differences between groups were determined using paired two-sided Student's *t*-test or two-way ANOVA. Pearson correlation test was used to determine the correlations between gene expressions, and survival analysis and a log-rank test was done by GraphPad Prism 5.0. A *P* value less than 0.05 was considered statistically significant compared with the controls, respectively.

Other detailed methods could be found in the supplementary methods.

Results

Hypoxia induces Bortezomib resistance in MM cells

Hypoxia has been known as a very important reason of drug resistance in ample solid tumors, therefore we investigated whether hypoxia influences the sensitivities of MM cells to drugs that have been shown effective in the clinic, such as Bortezomib (BTZ), carfizomib (CFZ), and melphalan (Mel). The sensitivity to BTZ of two MM cells, MM.1S and LP-1, were all obviously receded under hypoxia stimulus compare to the normoxia control (**Fig 1A, 1B**), as also shown by the significantly augmented half-maximal inhibitory concentration (IC_{50}) values (**Fig 1C**), the distinct abrogated cleavage of PARP as a marker of cell apoptosis (**Fig 1D**), and the remarkable suppressed apoptotic cell rates (**Fig 1E**). Intriguingly, hypoxia yielded the similar chemosensitivity alteration when treated another proteasome inhibitor Carfizomib (**Fig 1F-J**), but failed to induce conspicuous consequences of Melphalan in MM cells (**Fig 1K-O**). Thus, these results indicate that hypoxia more easily induces chemoresistance to protease inhibitor of MM cells.

Hypoxia upregulates SRC-3 level in MM cells

As our previous study has demonstrated high SRC-3 is associated with poor prognosis in MM, and overexpression of SRC-3 promotes BTZ resistance.[19] To dissert the correlation between SRC-3 and hypoxia, we assessed whether hypoxia affects SRC-3 expression in MM cells at mRNA or protein levels. We confirmed that hypoxia induced the augmentation at SRC-3 protein level in a time-dependent manner, neither coordinate with the alteration trend of HIF-1a, nor at mRNA level (**Fig 2A, 2B**). Immunofluorescence assay also validated that hypoxia promoted the accumulation of SRC-3 in the nucleus (**Fig 2A, 2B**). Similarly, high SRC-3 level was also found in our previously established bortezomib-resistant (BR) MM.1S and LP-1 cells compared with their parental cells (**Fig 2C, 2D**),[19,22] and administration of a newly developed small molecule targeting SRC-3, the SI-2,[23] partially rescued the sensitivity to BTZ of MM cells under hypoxia condition (**Fig 2E, 2F**). Importantly, combination of SI-2 and BTZ only showed synergistic anti-MM effect under hypoxia condition, but not in the normoxia controls, as evidenced by the remarkably augmented apoptotic cell rate and cleavage of PARP as a marker of cell apoptosis (**Fig 2G, 2H**). These data suggest that high SRC-3 protein provoked by hypoxia might be a critical regulator for sensitivity to PIs of MM cells.

Degradation of SRC-3 is ubiquitin-proteasome dependent

Since the augmentation of SRC-3 protein under hypoxia stimulus neither coordinate with HIF-1a level, nor occurred at transcriptional level, we speculate that hypoxia may enhance the stability of SRC-3 through another regulator. We assessed three major pathways governing protein degradation in MM cells, including the ubiquitin-proteasome pathway, lysosomal proteolysis and the calpain system. Therefore, we treated MM cells with different doses of MG132, Baf-A1, and MG101 for 24 hours, that are specific inhibitors for the above three pathways, respectively. The results showed that SRC-3 degraded mainly in a proteasome-dependent manner (**Fig S 1A-C**), which is similar with the alteration of SRC-3 in BTZ-treated MM cells (**Fig 3A**). We further used co-immunoprecipitation to confirm a physical association of SRC-3 and ubiquitin, and identified that SRC-3 was degraded mainly through lysine 11-(K11), K6-, and K29-linked polyubiquitination (**Fig 3C**). However, when the K6, K11, and K29 lysine residues of ubiquitin overexpressed in MM cells together with SRC-3, we only confirmed that SRC-3 protein was modified through K11-linked polyubiquitination, since we only elicited a dose-dependent modification of K11-linked polyubiquitination (**Fig 3D, 3E**) on SRC-3, but failed to observe the K6- and K29-linked polyubiquitination (**Fig 3F, 3G**). Moreover, when the K11 lysine was mutate to arginine, polyubiquitination of SRC-3 barely detected (**Fig 3H**). Thus, these results indicate that SRC-3 protein is mainly modified through K11-linked ubiquitination for degradation by the 26S proteasome.

SENP1 stabilizes SRC-3 through deSUMOylation

Next, we sought to deduct the key regulators for SRC-3 protein degradation through dissert the interactome of stably expressing flag-tagged SRC-3 MM.1S cells under hypoxia stimulation for 12 hours using mass spectrometry. Intriguingly, we did not find any E3 ligase in the components of SRC-3 interactome, on the contrary, we discovered a cysteine protease of the sentrin-specific protease (SENP) family, SENP1, which reverses SUMO conjugation on target proteins (**Fig 4A**). The interaction between

SRC-3 and SENP1 was confirmed by co-immunoprecipitation in the HEK293T cells, either using HA-SENP1 as bait protein to pulldown the SRC-3, or using Flag-SRC-3 as bait protein to pulldown SENP1, respectively (**Fig 4B**). Moreover, the endogenous interaction of SRC-3 and SENP1 was also validated in MM cells using anti-SRC-3 or anti-SENP1 antibodies, respectively (**Fig 4C**). In addition, protein level of SRC-3 was positively related to the exogenously expressed SENP1 in MM cells (**Fig S 2A**), and overexpression of SENP1 obviously prolonged the half-life of SRC-3 protein in MM cells (**Fig 4D**). These data suggested that degradation of SRC-3 might be regulated through coordination of SUMOylation and ubiquitination.

Previous studies have shown that transactivation activity of SRC-3 could be regulated by SUMOylation.[20] Actually, convergence of ubiquitination and SUMOylation in modulation of protein functions has emerged as a crucial cellular mechanism in regulating pathogenesis.[24] Our result showed that SRC-3 physically interacted with small ubiquitin-related modifier (SUMO)1, SUMO2, and SUMO3, but the interaction with SUMO1 was dominant (**Fig S 2B**). When SUMO1 was gradually overexpressed in MM cells, SRC-3 degradation was enhanced in a dose-dependent manner (**Fig S 2C**); on the contrary, SUMO1 depletion using lentivirus carrying shRNA resulted in attenuation of the SRC-3 ubiquitination (**Fig S 2D**). Thus, we confirmed that SUMOylation was involved in SRC-3 protein degradation. To further investigate the role of SUMOylation in SRC-3 stability *in vivo*, we generated a SUMO1 knockout mouse, and confirmed that SUMO1 has been completely depleted in B cells (**Fig S 2E**). In addition, the half-life of SRC-3 protein was markedly increased in the $SUMO1^{-/-}$ B cells (**Fig S 2F**), and ubiquitination of SRC-3 was barely detected in the $SUMO1^{-/-}$ B cells (**Fig 4H**). Taken together, these results suggest that SUMOylation was involved in proteasome-dependent degradation of SRC-3.

To further explore the role of SENP1 in SRC-3 modification, we knockdown SENP1 in the HEK293T cells that have stably expressed SUMO1 and flag-tagged SRC-3, and observed that SUMOylation of SRC-3 was markedly elevated (**Fig S 3A**); on the contrary, overexpression of SENP1 (SENP1-OE) remarkably attenuated the ubiquitination modification of SRC-3 compared with the vector controls (**Fig S 3B**). Importantly, overexpression of SENP1 dramatically relieved the K11-linked ubiquitination, but not K6- and K29-linked ubiquitination of SRC-3 (**Fig 4E**). To confirm the phenotype of SENP1 in regulating SRC-3 stability *in vivo*, we generated a SENP1 conditional knockout mouse model using SENP1-floxp and CD19-Cre crossed mice, and efficiently deleted SENP1 in the B cells (**Fig S 3C**). As a consequence, protein level of SRC-3 in the $SENP1^{fl/fl;\ CD19\text{-}Cre}$ B cells was obviously downregulated, and administration of MG132 failed to restore the protein level of SRC-3 compared with the B cells from wild type control mice (**Fig S 3D**). Moreover, the half-life of SRC-3 protein was markedly shortened in the $SENP1^{fl/fl;\ CD19\text{-}Cre}$ B cells compared with that in the wild type B cells (**Fig 4F**). As expected, endogenous ubiquitination and SUMOylation of SRC-3 was more readily detected in the $SENP1^{fl/fl;\ CD19\text{-}Cre}$ B cells but not in wild type B cells (**Fig 4G**). Collectively, our results indicate that SENP1 protects SRC-3 against degradation by SUMOylation-associated ubiquitination.

SENP1 is a downstream target of HIF-1a in MM cells

We next assessed how SENP1 was regulated by hypoxia in MM cells. Firstly, we tested expressions of the SENP family genes with HIF-1a overexpression (HIF-1a OE) in MM cells, and identified that hypoxia dominantly induced the expression of SENP1 in protein and mRNA level (**Fig 5A, 5B**), the results were similar under hypoxia condition in MM cells (**Fig 5C, 5D**). On the contrary, when HIF-1a was knockdown by lentivirus carrying shRNAs in MM cells (**Fig 5E**), SENP1 expression was dramatically suppressed both at mRNA and at protein levels, together with the downregulated SRC-3 only at protein level (**Fig 5F**). Interestingly, we verified the similar expression pattern of SENP1 in the BR-MM cells (**Fig 5G, 5H**). To determine whether HIF-1a is a transcriptional factor for *SENP1* promoter, we constructed a 2Kb SENP1 promoter, which contains two cis-acting elements of HIF-1a at -102~-111bp and -1684~-1691bp (**Fig 5I**), and ectopically expression of HIF-1a resulted in over 10 folds activation of the *SENP1*-luciferase reporter (**Fig 5J**). Importantly, hypoxia triggered significant enrichment of HIF-1a on SENP1 promoter in MM cells when detected by chromatin immunoprecipitation assay (**Fig 5K**). These results uncover that SENP1 is a direct target of HIF-1a under hypoxia condition.

SENP1 plays critical role in regulating chemosensitivity to PIs in MM cells

To further validate whether SENP1 is an important regulator of chemosensitivity in MM cells, we ectopically overexpressed (OE) or depleted the expression (KD) of SENP1 in MM.1S and LP-1 cells using lentivirus carrying expressing or shRNAs vectors, respectively (**Fig S 4A, 4B**). As expected, knockdown of SENP1 expression increased sensitivity to BTZ treatment in a dose-dependent manner, with a significantly reduced IC_{50} in both MM.1S and LP-1 cells (**Fig 6A, 6B**). Meanwhile, increased cell apoptosis due to BTZ treatment were observed in the SENP1-KD MM cells compared with the pared controls, as evidenced by augmented cleavage of PARP protein (**Fig 6C**), and apoptotic cell rates (**Fig 6D**). In contrast, overexpression of SENP1 in MM cells led to indolent response to BTZ treatment and inhibited cell apoptosis (**Fig 6E-H**). Importantly, suppression of SENP1 in the SRC-3 stably expressing MM cells using a specific inhibitor, Momordin Ic (Mc), remarkably sensitized the anti-MM efficacy of BTZ, but the synergetic effect of Mc failed to elicited in the SRC-3-KD MM cells (**Fig 6I, S 4C**). In addition, rescue of SRC-3 expression in the SENP1-KD MM cells largely reinstated the resistance to BTZ treatment compared with its paired vector control (**Fig 6J, S 4D**). Clinically, we observed that protein levels of HIF-1a, SENP1 and SRC-3 were mutually correlated, and the expressions were all significantly augmented in the refractory/relapsed MM patients (**Fig 6K, S 4E-H**), and combination of SENP1 inhibitor Mc with BTZ dramatically augmented cell apoptosis in primary CD138+ plasma cells that have been resistant to BTZ-based regiments (**Fig 6L**). In conclusion, these data suggest that SENP1 plays a critical role in regulating chemosensitivity to PIs in MM cells.

Targeting SENP1 suppresses hypoxia-induced SRC-3 and drug resistance in vivo

To assess the effect of targeting SENP1 in overcoming drug resistance *in vivo*, we established BTZ-resistant MM cell derived xenograft models, RRMM patient $CD138^+$ plasma cell derived intra-bone growth MM model, as well as the Vk*Myc transgenic and transplant mouse models of MM. The SENP1 inhibitor Mc alone administration had no obvious inhibitory effects on tumor growth, nor did BTZ alone

administration, however, the combination of BTZ and Mc considerably suppressed the tumor growth of MM (**Fig 7A**), prolonged the survival rate of mice (**Fig 7B**), and importantly, obviously more cell apoptosis (**Fig 7C**) and downregulated expression of SENP1 and SRC-3 were observed in the combined treatment groups (**Fig 7D**). Moreover, in three relapsed MM patients' bone marrow unsorted bone marrow mononuclear cells derived xenograft model, tumor burdens were also noticeably extenuated in the combination treatment groups, as evidenced by significantly suppressed M-protein levels (**Fig 7E**), and $CD138^+$ cells left in the bone marrow microenvironment (**Fig 7F**). Furthermore, in the successfully constructed Vk*Myc transplant mouse models of MM (**Fig S 5A-D**), we further validated the synergistic anti-MM effect of combination of SENP1 inhibitor and BTZ, as shown by the conspicuously reduced M-protein level (**Fig 7G**), increased survival rate of mice (**Fig 7H**), and nearly eradicated proportion of $CD138^+$ plasma cells in the bone marrow microenvironment (**Fig 7I**). Taken together, these in vivo data strongly suggest that pharmacologically targeting SENP1 abrogates chemoresistance to PIs in MM cells.

Discussion

In the current study, we identified an important role of hypoxia in regulating chemosensitivity to proteasome inhibitors of MM cells. Our study shows that hypoxia enhances SENP1 expression through the transcriptional factor HIF-1a, and the latter deSUMOylates SRC-3 via K11-linked ubiquitination, consequently protects the SRC-3 from 26S proteasome dependent degradation and favors MM cells survival and disease progression. Translationally, our pre-clinical data suggests that using small molecule targeting SENP1 could re-sensitize resistant MM cells to PIs, which may benefit the strategy development for refractory or relapsed MM patients.

Our previous findings has revealed that the histone methyltransferase NSD2 protects SRC-3 from degradation through forming liquid-liquid phase separation and renders resistance to PIs.[19] SRC-3 promotes numerous aspects of cancer, such as initiation, progression, and chemoresistance[25], and suppression of SRC-3 levels and/or activity are efficient enough to alter its transcriptome.[26,27] Several studies have demonstrated that stimuli could induce multiple posttranslational modifications of SRC-3, including phosphorylation, ubiquitination, SUMOylation, acetylation and methylation[25,28]. In this study, we report that hypoxia is a new stimulates for SRC-3 expression without affect its transcription level. Interestingly, we also discover that hypoxia mainly cause chemoresistance towards proteasome inhibitors, but not to other drugs such as Melphalan, a DNA alkylating drug inhibiting DNA and RNA synthesis.[29] Therefore, our study indicate that hypoxia may affect key regulators for chemosensitivity that dependents on the ubiquitin-proteasome system. Since SRC-3 is degraded in a proteasome-dependent manner, thus it is very easily affected by hypoxia.

After deciphering the interactome of SRC-3 in MM cells under hypoxia condition, we unexpectedly discovered a deSUMOylation enzyme SENP1, but no ubiquitination related E3 ligase. SENP1 belongs to SUMO-specific proteases (SENPs), which have a dual function as processing enzymes for pre-SUMO and deconjugates of SUMO conjugates[30]. Although SENPs are known to reverse SUMOylation in many

different systems, their physiological role has not been precisely defined. Overexpression of SENP1 positively correlated with clinicopathological features such as tumor differentiation, lymph node metastasis, cancer aggressiveness, and recurrence.[31,32] Similar to its roles in solid tumors, our study demonstrates that SENP1 is an important regulator for chemoresistance to PIs in MM cells under hypoxia condition.

Small ubiquitin-like modifiers (SUMOs) are conservatively expressed in all eukaryotes, engender protein SUMOylation modification, and are essential for the maintenance of genomic integrity and the regulation of gene expression and intracellular signaling[33]. SUMO chains serve as targeting signals recognized by members of a novel class of ubiquitin ligases termed SUMO-targeted ubiquitin ligases (STUbL) or ubiquitin ligases (E3) for sumoylated proteins (ULS, E3-S). There are varies result for sumoylated proteins.[34] For example, ULSs mediate ubiquitination of sumoylated proteins for degradation by the proteasome, and ULSs seem to generate a novel composite binding motif recognized by tandem ubiquitin and SUMO interaction motifs[34,35]. Our present study provides the first evidence that SUMOylation coordinates with ubiquitination in regulating the stability of SRC-3, providing a novel knowledge for understanding the regulation of SRC-3 stability in MM cells under hypoxia condition. In solid tumors, it has been well established that hypoxia has a negative effect on the efficacy of radio- and chemotherapy, through affecting drug delivery, DNA damage repair, regulation of genes governing drug resistance, as well as cell death pathways.[36,37] The bone marrow microenvironment which has been invaded by MM cells contains a heterogeneous range of oxygen pressures due to imbalanced rapidly proliferating cells and angiogenesis, but the average oxygen pressure generally is under the normoxia range. In this study, we provided evidences that hypoxia promotes the transcription of SENP1 through HIF-1a, and protects SRC-3 protein against degradation by SUMOylation-mediated ubiquitination.

In summary, this study provides new knowledge for understanding the underlying mechanism of resistance to PIs under hypoxia condition, and further emphasizes the importance of SRC-3 in regulating sensitivity to PIs via the linkage of its interaction with the SUMO-specific protease SENP1. Our results also shed light on guiding the development of therapeutic strategies to overcome refractory or relapse in MM patients using the SENP1 inhibitor in clinic.

Declarations

Acknowledgement

We thank Dr. Leif Bergsagel at the Mayo Clinic for kindly providing the Vk*Myc mouse spleen cells. This work was supported by the National Natural Science Foundation of China (81870161, 82070221, ZQ Liu; 81900215, JY Wang; 81870150, ZG Zhao), the Tianjin Research Innovation Project for Postgraduate Students (2020YJSB162, Y.X.), and the Beijing Natural Science Foundation of China (Z200020, ZQ Liu).

Author contributions

L.G. and ZQ.L. contributed to writing the manuscript; J.G., YY.L., S.W., Y.X., HM.J., X.L., ZY.P., YX.W., and J.P. M. contributed to performing the experiments and statistical analyses; J.G., S.W., ML.H. and MQ.W. were in charge of the animal studies; ZG.Z. and XK.C. provided the patient samples and clinical statistics; ZQ.L. and ZG. Z. contributed to the final version of the manuscript.

Competing interests

All authors declare no competing interests.

Data availability statement

All data needed to evaluate the conclusions in the paper are present in the paper and/or the Supplementary Materials. Source data are provided with this paper. Requests for any materials in this study should be directed to Zhiqiang Liu and obtained through an MTA.

Consent for publication

All authors concur with the submission and publication of this research article.

References

1. van de Donk N, Pawlyn C, Yong KL. Multiple myeloma. Lancet. 2021;397(10272):410–427.
2. Moser-Katz T, Joseph NS, Dhodapkar MV, Lee KP, Boise LH. Game of Bones: How Myeloma Manipulates Its Microenvironment. Front Oncol. 2020;10:625199.
3. Kumar SK, Rajkumar V, Kyle RA, et al. Multiple myeloma. Nat Rev Dis Primers. 2017;3:17046.
4. From the American Association of Neurological Surgeons ASoNC, Interventional Radiology Society of Europe CIRACoNSESoMINTESoNESOSfCA, Interventions SoIRSoNS, et al. Multisociety Consensus Quality Improvement Revised Consensus Statement for Endovascular Therapy of Acute Ischemic Stroke. *Int J Stroke*. 2018;13(6):612–632.
5. Ikeda S, Tagawa H. Impact of hypoxia on the pathogenesis and therapy resistance in multiple myeloma. Cancer Sci. 2021;112(10):3995–4004.
6. Ria R, Vacca A. Bone Marrow Stromal Cells-Induced Drug Resistance in Multiple Myeloma. Int J Mol Sci. 2020;21(2).
7. Kawano Y, Moschetta M, Manier S, et al. Targeting the bone marrow microenvironment in multiple myeloma. Immunol Rev. 2015;263(1):160–172.
8. Yen CH, Hsiao HH. NRF2 Is One of the Players Involved in Bone Marrow Mediated Drug Resistance in Multiple Myeloma. Int J Mol Sci. 2018;19(11).
9. Pennathur-Das R, Levitt L. Augmentation of in vitro human marrow erythropoiesis under physiological oxygen tensions is mediated by monocytes and T lymphocytes. Blood. 1987;69(3):899–907.

10. Danet GH, Pan Y, Luongo JL, Bonnet DA, Simon MC. Expansion of human SCID-repopulating cells under hypoxic conditions. J Clin Invest. 2003;112(1):126–135.
11. Hu J, Handisides DR, Van Valckenborgh E, et al. Targeting the multiple myeloma hypoxic niche with TH-302, a hypoxia-activated prodrug. Blood. 2010;116(9):1524–1527.
12. Martin SK, Diamond P, Gronthos S, Peet DJ, Zannettino AC. The emerging role of hypoxia, HIF-1 and HIF-2 in multiple myeloma. Leukemia. 2011;25(10):1533–1542.
13. Xu Y, Guo J, Liu J, et al. Hypoxia-induced CREB cooperates MMSET to modify chromatin and promote DKK1 expression in multiple myeloma. Oncogene. 2021;40(7):1231–1241.
14. Yuen VW, Wong CC. Hypoxia-inducible factors and innate immunity in liver cancer. J Clin Invest. 2020;130(10):5052–5062.
15. de Heer EC, Jalving M, Harris AL. HIFs, angiogenesis, and metabolism: elusive enemies in breast cancer. J Clin Invest. 2020;130(10):5074–5087.
16. Mani DR, Krug K, Zhang B, et al. Cancer proteogenomics: current impact and future prospects. Nat Rev Cancer. 2022.
17. Lothrop AP, Torres MP, Fuchs SM. Deciphering post-translational modification codes. FEBS Lett. 2013;587(8):1247–1257.
18. Wirth M, Schick M, Keller U, Kronke J. Ubiquitination and Ubiquitin-Like Modifications in Multiple Myeloma: Biology and Therapy. Cancers (Basel). 2020;12(12).
19. Liu J, Xie Y, Guo J, et al. Targeting NSD2-mediated SRC-3 liquid-liquid phase separation sensitizes bortezomib treatment in multiple myeloma. Nat Commun. 2021;12(1):1022.
20. Wu H, Sun L, Zhang Y, et al. Coordinated regulation of AIB1 transcriptional activity by sumoylation and phosphorylation. J Biol Chem. 2006;281(31):21848–21856.
21. Chesi M, Matthews GM, Garbitt VM, et al. Drug response in a genetically engineered mouse model of multiple myeloma is predictive of clinical efficacy. Blood. 2012;120(2):376–385.
22. Wang J, Zhu X, Dang L, et al. Epigenomic reprogramming via HRP2-MINA dictates response to proteasome inhibitors in multiple myeloma with t(4;14) translocation. J Clin Invest. 2022;132(4).
23. Song X, Chen J, Zhao M, et al. Development of potent small-molecule inhibitors to drug the undruggable steroid receptor coactivator-3. Proc Natl Acad Sci U S A. 2016;113(18):4970–4975.
24. Kumar R, Sabapathy K. RNF4-A Paradigm for SUMOylation-Mediated Ubiquitination. Proteomics. 2019;19(21–22):e1900185.
25. Li L, Deng CX, Chen Q. SRC-3, a Steroid Receptor Coactivator: Implication in Cancer. Int J Mol Sci. 2021;22(9).
26. Geng C, Rajapakshe K, Shah SS, et al. Androgen receptor is the key transcriptional mediator of the tumor suppressor SPOP in prostate cancer. Cancer Res. 2014;74(19):5631–5643.
27. Lanz RB, Bulynko Y, Malovannaya A, et al. Global characterization of transcriptional impact of the SRC-3 coregulator. Mol Endocrinol. 2010;24(4):859–872.

28. Xu J, Wu RC, O'Malley BW. Normal and cancer-related functions of the p160 steroid receptor co-activator (SRC) family. Nat Rev Cancer. 2009;9(9):615–630.
29. Mougenot P, Bressolle F, Culine S, Solassol I, Poujol S, Pinguet F. In vitro cytotoxic effect of melphalan and pilot phase II study in hormone-refractory prostate cancer. Anticancer Res. 2006;26(3B):2197–2203.
30. Kunz K, Piller T, Muller S. SUMO-specific proteases and isopeptidases of the SENP family at a glance. J Cell Sci. 2018;131(6).
31. Ma C, Wu B, Huang X, et al. SUMO-specific protease 1 regulates pancreatic cancer cell proliferation and invasion by targeting MMP-9. Tumour Biol. 2014;35(12):12729–12735.
32. Xiang-Ming Y, Zhi-Qiang X, Ting Z, et al. SENP1 regulates cell migration and invasion in neuroblastoma. Biotechnol Appl Biochem. 2016;63(3):435–440.
33. Chang HM, Yeh ETH. SUMO: From Bench to Bedside. Physiol Rev. 2020;100(4):1599–1619.
34. Sriramachandran AM, Dohmen RJ. SUMO-targeted ubiquitin ligases. Biochim Biophys Acta. 2014;1843(1):75–85.
35. Chang YC, Oram MK, Bielinsky AK. SUMO-Targeted Ubiquitin Ligases and Their Functions in Maintaining Genome Stability. Int J Mol Sci. 2021;22(10).
36. Scanlon SE, Glazer PM. Multifaceted control of DNA repair pathways by the hypoxic tumor microenvironment. DNA Repair (Amst). 2015;32:180–189.
37. Rohwer N, Cramer T. Hypoxia-mediated drug resistance: novel insights on the functional interaction of HIFs and cell death pathways. Drug Resist Updat. 2011;14(3):191–201.

Figures

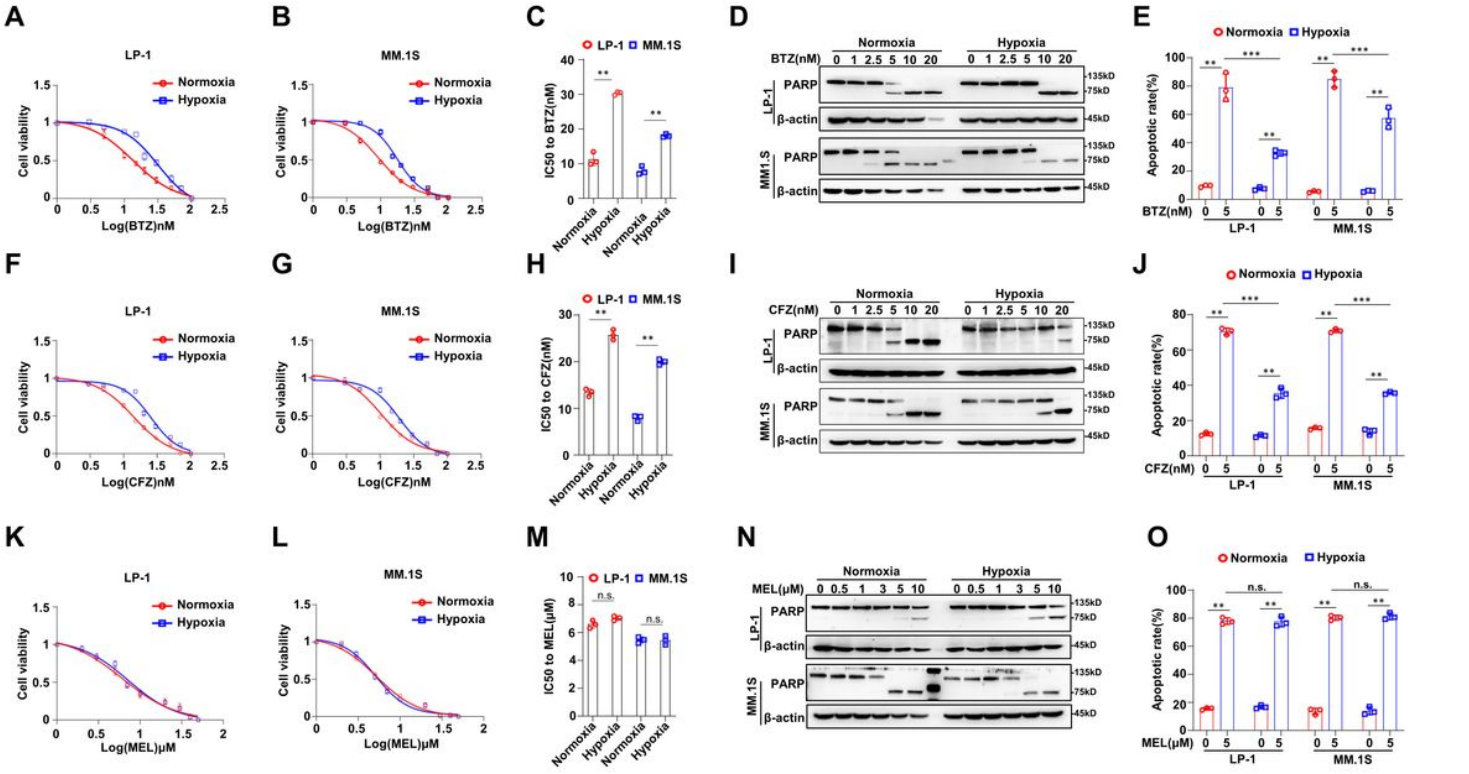

Figure 1

Figure 1

Hypoxia induces Bortezomib resistance in MM cells

(A⊠B⊠C) Alteration of IC_{50} to BTZ treatment under hypoxia and normoxia condition for 48 hr in LP-1 and MM.1S cells. **(D)** Cleavage of PARP as the apoptotic marker in MM cells under hypoxia and normoxia condition, treated with increasing dosage of bortezomib (BTZ) for 48 hr. **(e)** Flo w cytometry assay for apoptosis of LP-1 and MM.1S MM cells under hypoxia and normoxia condition induced by 5 nM BTZ for 48 hr. **(f, g, h)** Alteration of IC_{50} to CFZ treatment under hypoxia and normoxia condition for 48 hr in LP-1 and MM.1S cells. **(i)** Cleavage of PARP as the apoptotic marker in MM cells under hypoxia and normoxia condition, treated with increasing dosage of Carfilzomib (CFZ) for 48 hr. **(J)** Flow cytometry assay for apoptosis of LP-1 and MM.1S cells under hypoxia and normoxia condition induced by 5 nM CFZ for 48 hr. **(K, L, M)** Alteration of IC_{50} to MEL treatment under hypoxia and normoxia condition for 48 hr in LP-1 and MM.1S cells. **(N)** Cleavage of PARP as the apoptotic marker in MM cells under hypoxia and normoxia condition, treated with increasing dosage of Melphalan (MEL) for 48 hr. **(O)** Flow cytometry assay for apoptosis of LP-1 and MM.1S cells induced by 5 μM MEL for 48 hours. *$P < 0.05$, **$P < 0.01$, ***$P < 0.001$, two-sided P values were determined by Student's t test for n = 3 biologically independent experiments.

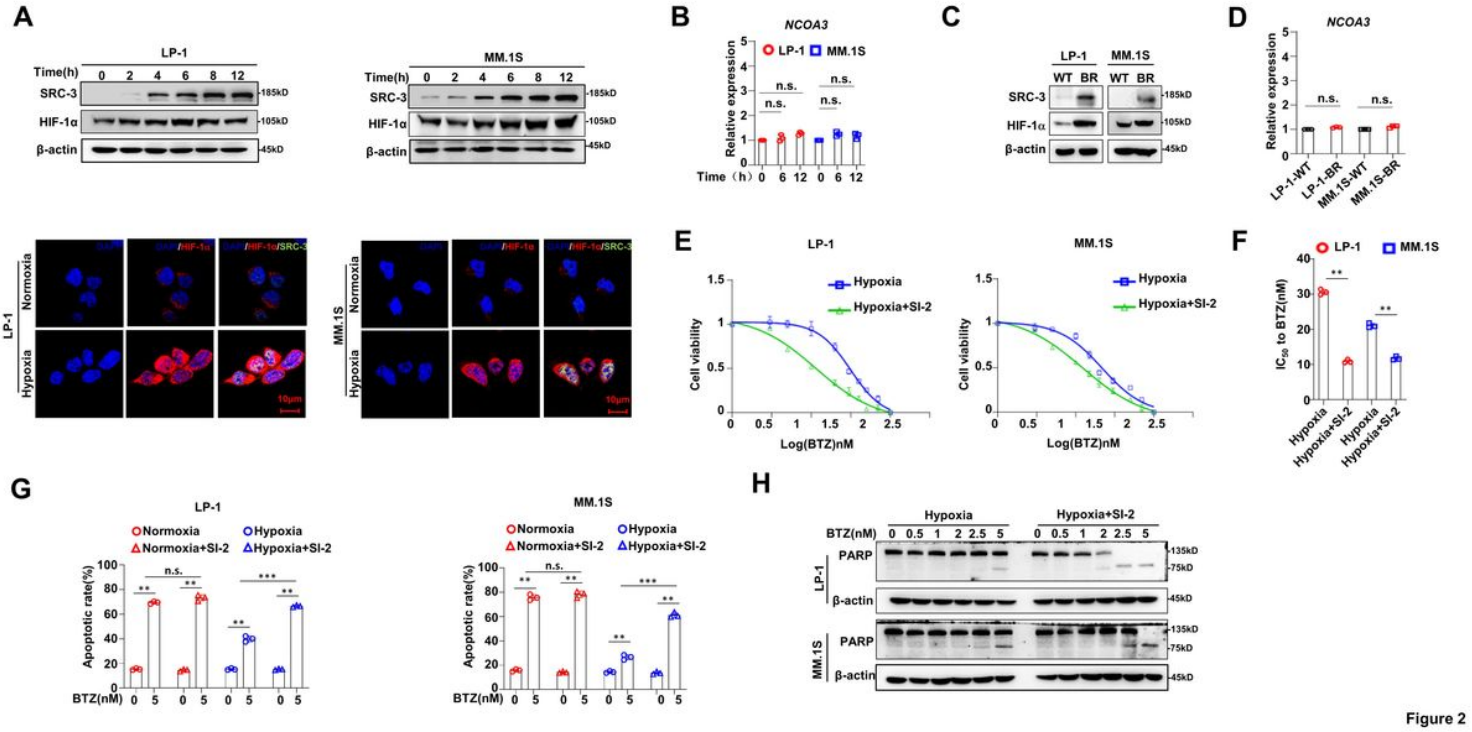

Figure 2

Figure 2

Hypoxia upregulates SRC-3 level in MM cells

(**a**) Western Blotting and immunofluorescence to test the levels of SRC-3, HIF-1a in LP-1 and MM.1S cells under hypoxia and normoxia in indicated time. Scale bar, 10 μm. (**B**) qPCR shows the expression of *NCOA3* in LP-1 and MM.1S cells - under hypoxia condition with indicated time. (**C**) Western Blotting shows b-actin SRC-3, HIF-1α expressions in wild type (WT) and bortezomib (BTZ)-resistant (BR) MM cells. (**D**) qPCR shows the expression of *NCOA3* in WT and BR-MM cells. (**E, F**)Alteration of IC_{50} to BTZ treatment under hypoxia condition in the presence or absence of 25 nM SI-2 for 48 hr in LP-1 and MM.1S cells (**G**) Flow cytometry assay for apoptosis of LP-1 and MM.1S cells induced by 5 nM BTZ in the presence or absence of 25 nM SI-2 for 48 hr. (**H**) Cleavage of PARP as the apoptotic marker in MM cells under hypoxia condition in the presence or absence of 25 nM SI-2 for 48 h, treated with increasing dosage of BTZ for 48 hr. **P* < 0.05, ***P* < 0.01, ****P* < 0.001, two-sided *P* values were determined by Student's t test for n = 3 biologically independent experiments.

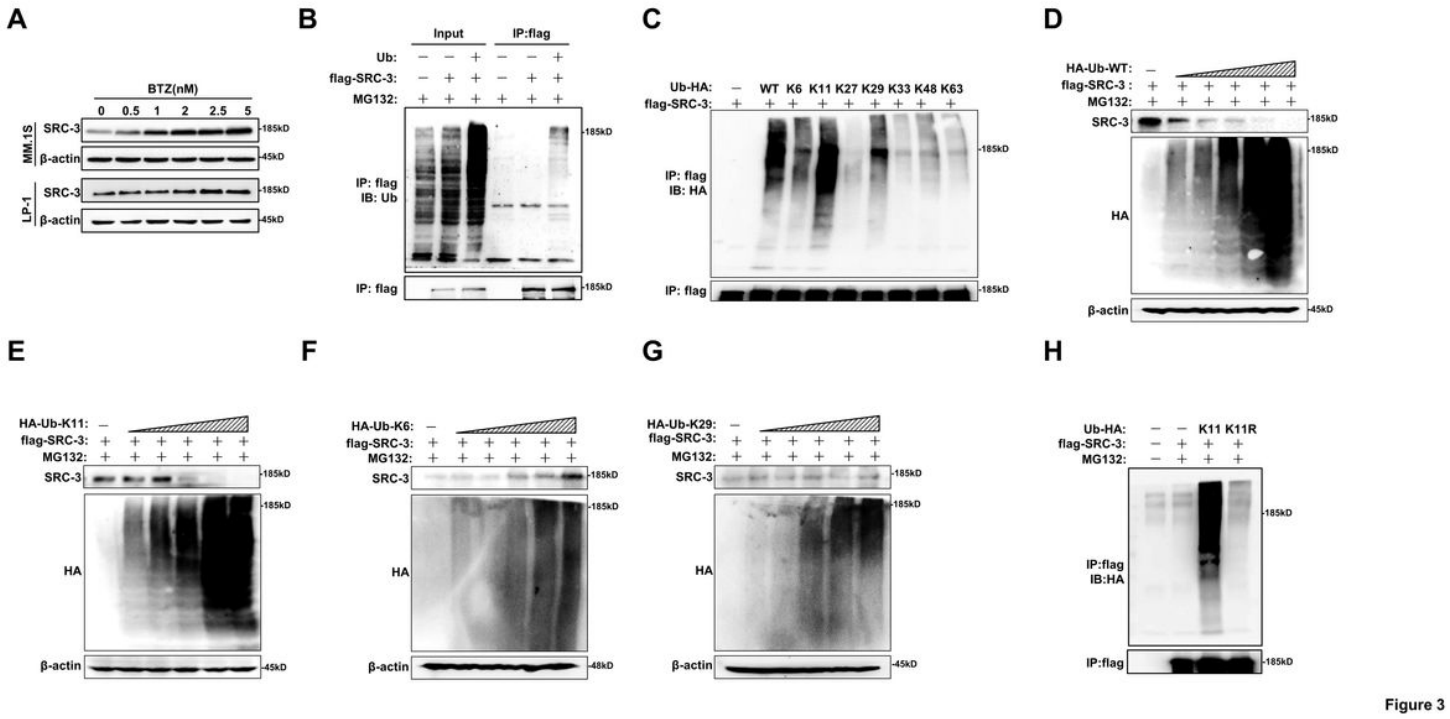

Figure 3

Degradation of SRC-3 is ubiquitin-proteasome dependent

(**a**) Levels of SRC-3 in LP-1 and MM.1S cells treated with increasing dosage of BTZ for 24 hr. (**b**) Co-immunoprecipitation (Co-IP) assay shows interactions between Ubiquitination and SRC-3. Input, 2% lysate. IP, M2-flag antibody. (**c**) Co-IP assay shows the interactions between Ub-WT, Ub-K6, Ub-K11, Ub-K27, Ub-K29, Ub-K33, Ub-K48, Ub-K63 and SRC-3. Input, 2% lysate. IP, M2-flag antibody. (**D**) SRC-3-3×flag levels in HEK293T cells co-transfected with Ub-WT for 48 hr and treated with MG132 (10 mM) for 4 hr before harvesting proteins were detected by anti-flag immunoblotting (IB). (**E**) SRC-3-3×flag levels in HEK293T cells co-transfected with Ub-K11 for 48 hr and treated with MG132 (10 mM) for 4 hr before harvesting proteins were detected by anti-flag IB. (**F**) SRC-3-3×flag levels in HEK293T cells co-transfected with Ub-K6 for 48 hr and treated with MG132 (10 mM) for 4 hr before harvesting proteins were detected by anti-flag IB. (**G**) SRC-3-3×flag levels in HEK293T cells co-transfected with Ub-K29 for 48 hr and treated with MG132 (10 mM) for 4 hr before harvesting proteins were detected by anti-flag IB. (**H**) Co-IP assay shows interactions between SRC-3 and Ub-K11 or Ub-K11R . Input, 2% lysate. IP, M2-flag antibody.

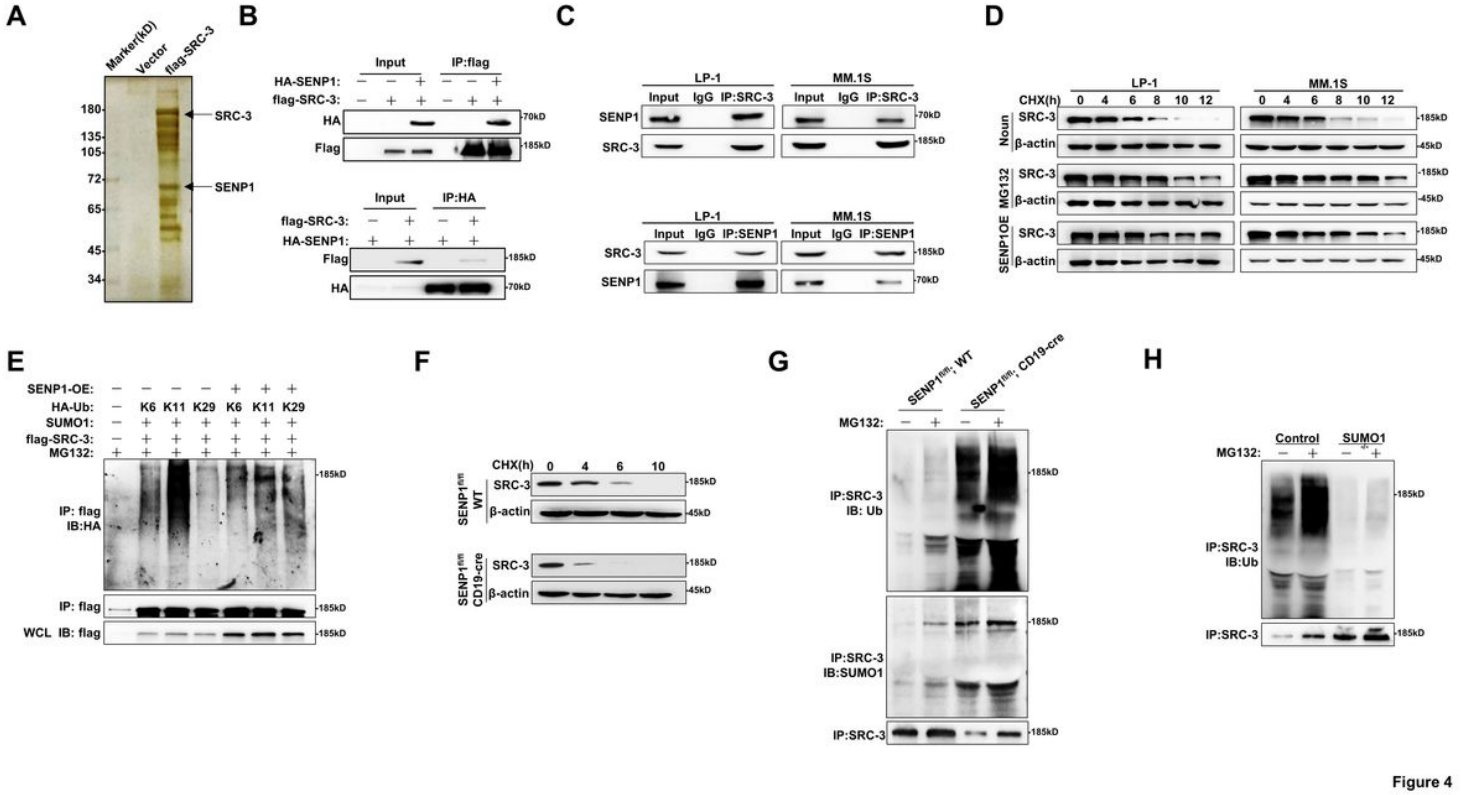

Figure 4

Figure 4

SENP1 stabilize SRC-3 through deSUMOylation

(**a**) Silver staining of MM.1S cells infected with lentivirus carrying SRC-3-3×flag for 72 hr and then under hypoxia stimulation for 12 hr. (**b**) Interaction between exogenous FLAG-SRC-3 and HA-SENP1 in HEK 293T cells was detected by Co-IP using anti-flag antibody, and reversely IP using anti-HA antibody after co-transfection for 48hr. (**c**) Interaction between endogenous SRC-3 and SENP1 in MM.1S and LP-1 cells was detected by using SRC-3 antibody or reversely SENP1 antibody for IP. (**d**) Degradation of SRC-3 in MM.1S and LP-1 cells treated with or without MG132 and with or without SENP1 overexpression. (**e**)Indicated plasmids were co-transfected in HEK 293T cells and treated with MG132 (10 mM) for 4 hr before harvesting protein, immunoprecipitated with anti-flag antibody. Bound proteins were detected by anti-HA IB. **(f)** The half-life of SRC-3 protein was decreased in SENP1$^{fl/fl}$, CD19-cre B cells. **(g)** SUMOylation level of SRC-3 accumulated in SENP1$^{fl/fl}$, CD19-cre B cells after treated with MG132. SENP1$^{fl/fl}$, CD19-cre and SENP1$^{fl/fl}$ B cells were treated with MG132 (10mM) for 4 hr as indicated. SRC-3 was immunoprecipitated with anti-SRC-3 antibody from cell lysates. The precipitates were immunoblotted (IB) with anti-Ub, anti-SUMO1 antibodies. **(h)** Ubiquitination of SRC-3 accumulated in Control B cells after treated with MG132. SUMO1$^{-/-}$ and Control B cells were treated MG132 (10 mM) for 4 hr as indicated. SRC-3 was immunoprecipitated with anti-SRC-3 antibody from cell lysates. The precipitates were immunoblotted (IB) with anti-Ub antibodies.

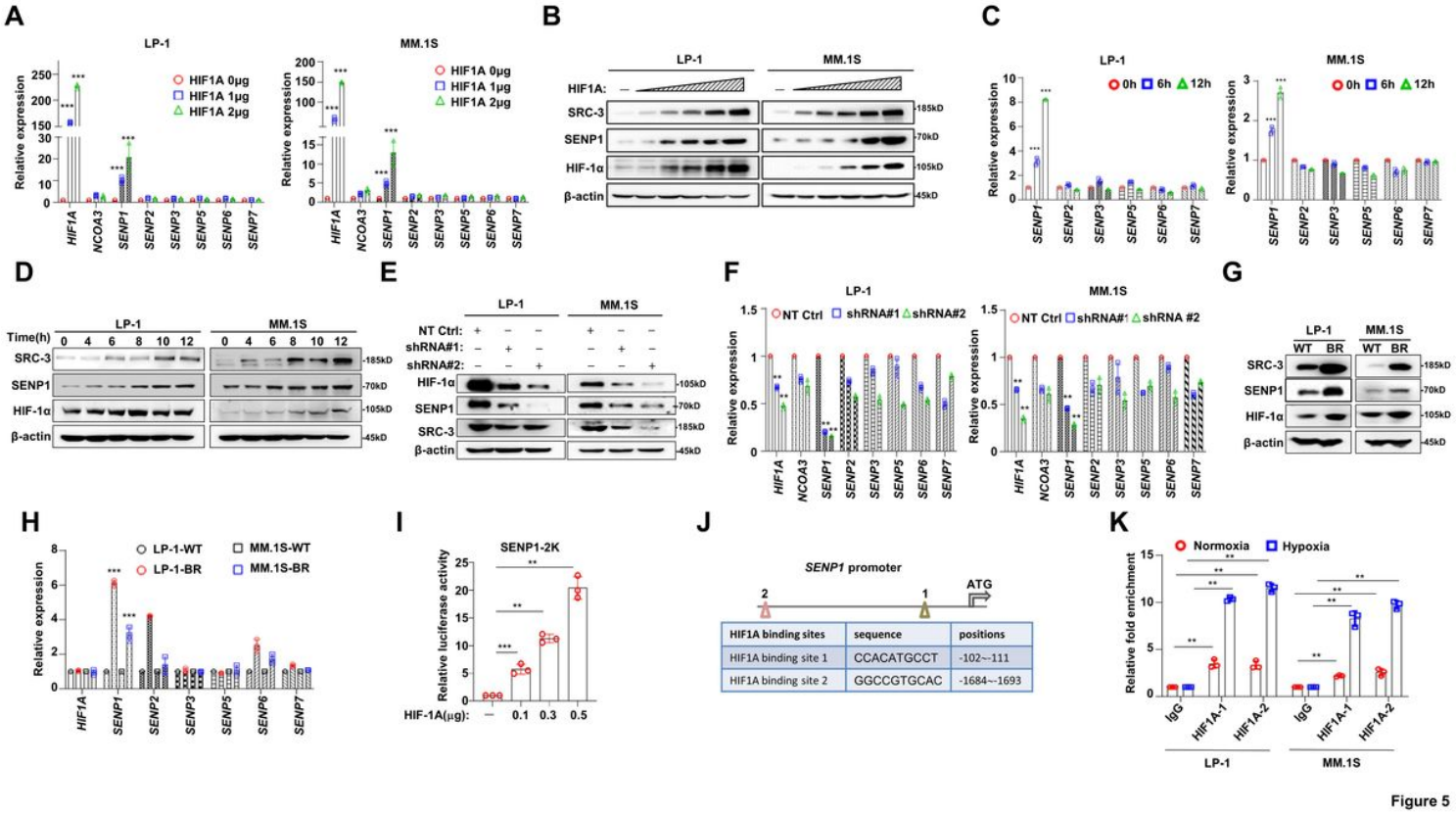

Figure 5

Figure 5

SENP1 is a downstream target of HIF-1a in MM cells

(a) qPCR shows indicated gene expressions in LP-1 and MM.1S cells transfected with HIF-1α with indicated amount. **(B)** Levels of SENP1 in LP-1 and MM.1S cells transfected with increasing dosage of HIF-1α lentivirus for 48 hr. **(C)** qPCR shows indicated gene expressions in LP-1 and MM.1S cells under hypoxia for indicated time. **(D)** Levels of SRC-3, SENP1, HIF-1α in LP-1 and MM.1S cells under hypoxia condition in indicated time. **(E)** Levels of HIF-1α, SENP1, SRC-3 in the NT Ctrl and HIF-1α knockdown (KD) LP-1 and MM.1S cells. **(F)** qPCR shows indicated gene expressions in the NT Ctrl and HIF-1α KD LP-1 and MM.1S cells. (**G**) Western Blotting shows SENP1, SRC-3, HIF-1α expressions in WT and BR-MM cells. (**H**) qPCR shows indicated gene expressions in WT and BR MM cells. **(I)** Luciferase assay shows the activity of pGL3-*SENP1*-luc reporter in the presence of increasing HIF-1α overexpression plasmid (HIF-1α-OE), pGL3-basic vector was used as control. **(J)** Schematic illustration of the site of HIF-1α binding to the promoter of SENP1. **(K)** ChIP-qPCR profile for 2 clusters of genes enriched by SENP1 in MM.1S and LP-1 cells under normoxia and hypoxia condition. **P* < 0.05, ***P* < 0.01, ****P* < 0.001, two-sided *P* values were determined by Student's t test for n = 3 biologically independent experiments.

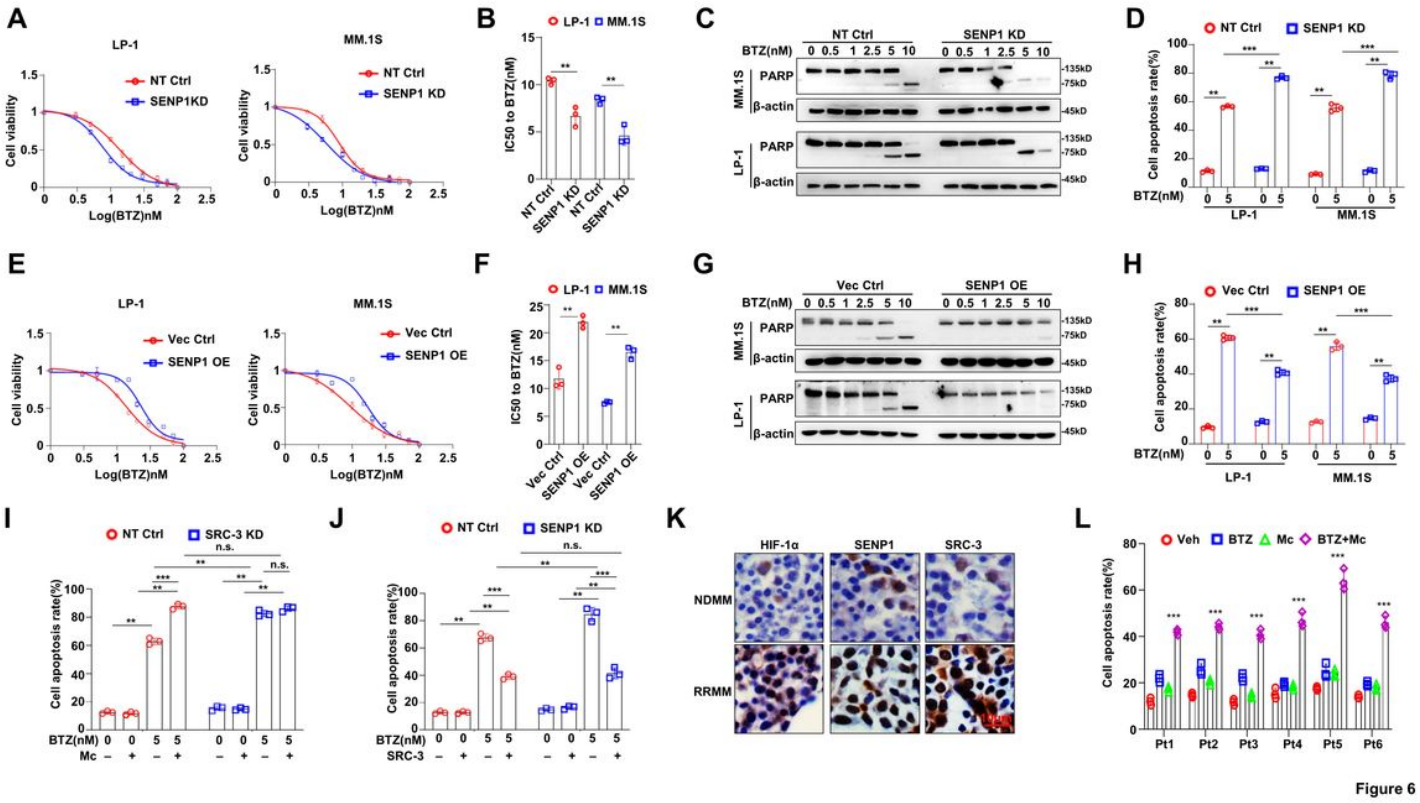

Figure 6

Figure 6

SENP1 plays critical role in regulating chemosensitivity to PIs in MM cells

(a, B) Alteration of IC_{50} to BTZ treatment in the NT Ctrl and SENP1-KD of MM cells. **(C)** Cleavage of PARP in MM cells with SENP1 expression manipulated by shRNA, treated with increasing dosage of BTZ for 48 hr. **(D)** Flow cytometry assay for apoptosis of MM cells in the NT Ctrl and SENP1-KD cells and induced by 5 nM BTZ for 48 hr. **(E, F)** Alteration of IC_{50} to BTZ treatment in the SENP1-OE or control MM cells. (**G**) Cleavage of PARP in the SENP1-OE or control MM cells treated with increasing dosage of BTZ for 48 hr. (**H**) Flow cytometry assay for apoptosis SENP1-OE or control MM cells induced by 5 nM BTZ for 48 hr. **(i)** Flow cytometry analysis for apoptosis of SRC-3-KD or control MM.1S cells treated with increasing dosage of BTZ (5nM) and 25 μM Mc for 48 hr. **(J)** Flow cytometry analysis for apoptosis of SENP1-KD or control MM.1S cells treated with increasing dosage of BTZ with or without SRC-3 knockdown. **(K)** Immunohistochemical images of bone marrow biopsies from newly developed (NDMM) or refractory/relapsed (RRMM) MM patients. Scale bar, 10 mm. **(L)** Flow cytometry analysis for apoptosis of $CD138^+$ plasma cells from MM patients with relapse after BTZ-based treatments. PCs were cultured on bone marrow stromal cells and treated with BTZ (5 nM) and Mc (25 μM) for 12 h. $^*P < 0.05$, $^{**}P < 0.01$, $^{***}P < 0.001$, two-sided *P* values were determined by Student's t test for n = 3 biologically independent experiments.

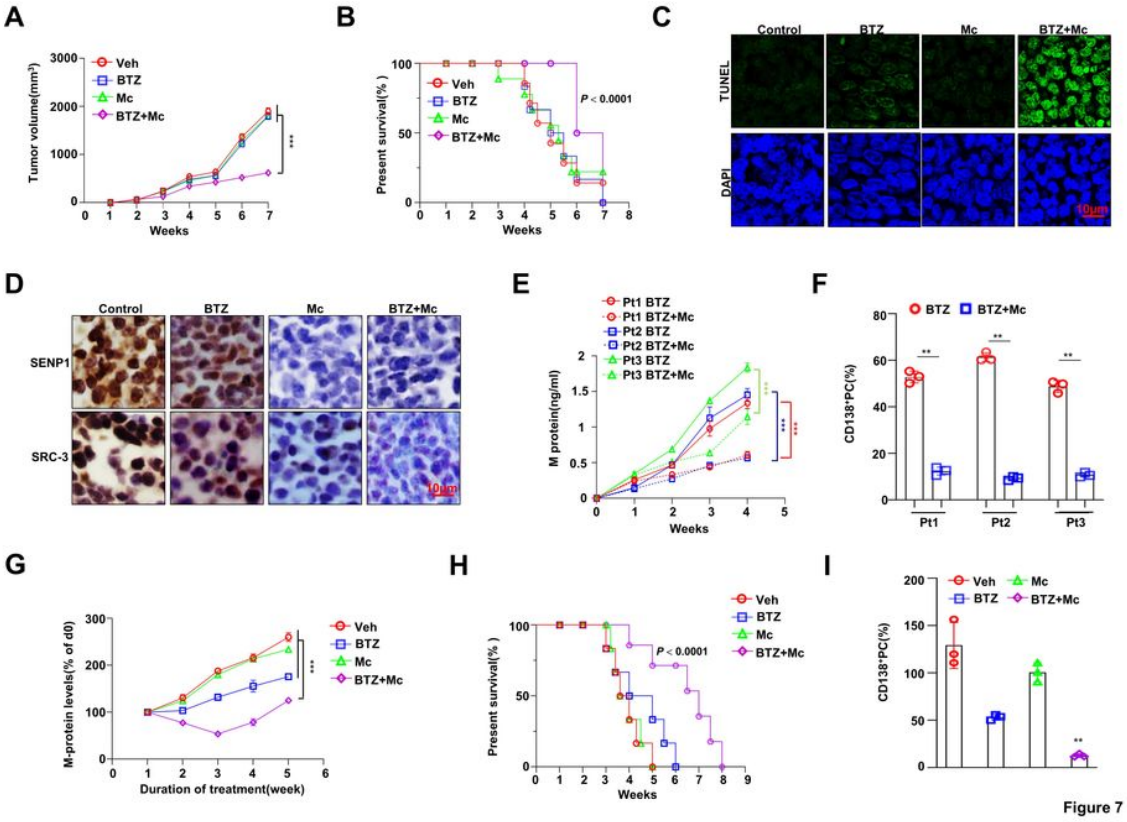

Figure 7

Targeting SENP1 in myeloma cells attenuates hypoxia induced SRC-3 expression and drug resistance.

(a) Tumor growth of BR LP-1 cells (3×10^6 cells/mouse) in NSG mice combined treatment with DMSO, BTZ, Mc or BTZ plus Mc (n = 6 mice/ group). **(b)** Survival of mice at the time point of tumor size = 15 mm^3 (n = 6 mice /group). **(c, d)** Representative micrographs (n = 12 biologically independent samples) of immunohistochemistry staining in tissues from xenograft of mice treated with BTZ, Mc or BTZ plus Mc to detect SRC-3 level and apoptosis using TUNEL kit. Scale bar, 10 mm. **(e)** Levels of M-protein secreted by patient derived MM cells in the inoculated NSG mice tail venous blood after treated with BTZ or combined with Mc (n = 6 mice/patient, n = 3 mice/group). **(f)** Percentage of human $CD138^+$ cells in the bone marrow of NSG mice after receiving 3 weeks of BTZ or BTZ combined with Mc treatment. n = 6 mice/patient sample, n = 3 mice/group. **(g)** Vk*MYC mice were treated with Mc (10 mg/kg, third weekly, n= 6), BTZ (1 mg/Kg, third weekly, n= 6), the combination of both drugs (n= 6) or vehicle control (DMSO, n=7) for 4 weeks. Serum paraprotein was assessed on day 1 and then weekly for 5 weeks and presented as mean change from levels on day 0 (mean SEM). **(h)** Survival of Vk*MYC mice treated with Mc, BTZ, the combination of both drugs and DMSO. (**G**) FACS analysis of $CD138^+/B220^-$PCs in the BM of Vk*MYC mice after 5 days of treatment with Mc, BTZ, the combination of both drugs or DMSO. Values are normalized to the percentage of PCs in vehicle control treated BM (100%). *$P < 0.05$, **$P < 0.01$, ***$P < 0.001$, two-sided P value determined by Student's t test; mean ± SD of 3 independent experiments.

Supplementary Files

This is a list of supplementary files associated with this preprint. Click to download.

- SupplementaryFigures15.pdf
- Supplymentarymethod.pdf